

Implementation scheme for quantum controlled phase-flip gate through quantum dot in slow-light photonic crystal waveguide

Jie Gao, F. W. Sun, and Chee Wei Wong

Citation: *Appl. Phys. Lett.* **93**, 151108 (2008); doi: 10.1063/1.2999588

View online: <http://dx.doi.org/10.1063/1.2999588>

View Table of Contents: <http://apl.aip.org/resource/1/APPLAB/v93/i15>

Published by the [American Institute of Physics](http://www.aip.org).

Related Articles

Electromagnetically induced transparency with quantum interferometry

J. Chem. Phys. **136**, 084301 (2012)

Huge enhancement of optical nonlinearities in coupled Au and Ag nanoparticles induced by conjugated polymers

Appl. Phys. Lett. **100**, 023106 (2012)

Spatial hole burning degradation of AlGaAs/GaAs laser diodes

Appl. Phys. Lett. **99**, 103506 (2011)

Optical limiting properties and ultrafast dynamics of six-branched styryl derivatives based on 1,3,5-triazine

J. Appl. Phys. **110**, 033518 (2011)

Plasmon induced transparency in a dielectric waveguide

Appl. Phys. Lett. **99**, 043113 (2011)

Additional information on *Appl. Phys. Lett.*

Journal Homepage: <http://apl.aip.org/>

Journal Information: http://apl.aip.org/about/about_the_journal

Top downloads: http://apl.aip.org/features/most_downloaded

Information for Authors: <http://apl.aip.org/authors>

ADVERTISEMENT



LakeShore Model 8404 developed with **TOYO Corporation**
NEW AC/DC Hall Effect System Measure mobilities down to 0.001 cm²/V s

Implementation scheme for quantum controlled phase-flip gate through quantum dot in slow-light photonic crystal waveguide

Jie Gao,^{a)} F. W. Sun, and Chee Wei Wong^{a)}

Optical Nanostructures Laboratory, Columbia University, New York, New York 10027, USA

(Received 20 April 2008; accepted 16 September 2008; published online 14 October 2008)

We propose a scheme to realize controlled phase gate between two single photons through a single quantum dot in a slow-light photonic crystal waveguide. Enhanced Purcell factor and large β -factor lead to high gate fidelity over broadband frequencies compared to cavity-assisted system. The excellent physical integration of this photonic crystal waveguide system provides tremendous potential for large-scale quantum information processing. © 2008 American Institute of Physics. [DOI: 10.1063/1.2999588]

The atom-cavity system has been examined as a critical component for quantum information processing, including demonstrations of the single photon source,¹ two-qubit quantum gate operation,^{2,3} and entanglement generation.⁴ Using a cavity to modify the local density of states (LDOS), however, the qubit operation is typically limited to a narrow-band spectral region, in addition to photon extraction, scalability, and integrability issues that need to be carefully considered. Alternatively, other possible mesoscopic structures to increase the LDOS include one-dimensional slow-light photonic crystal (PhC) waveguides⁵ and surface plasmon waveguides. Such systems have been theoretically proposed recently to achieve single photon transistors and single photon sources.^{6,7} Remarkable observations such as enhanced spontaneous emission⁸ and strong coupling seen in mesoscopic microcavities can also be ported into the PhC waveguide or nanowire system. For instance, signatures of spontaneous emission enhancement with ensemble quantum dots (QDs) in a PhC waveguide have recently been observed.⁹ In this Letter, we propose a system which consists of photonic crystal waveguides and low dimensional semiconductor QD for implementing the controlled phase-flip (CPF) gate between two flying qubits. We further show that enhanced QD emission into PhC waveguide mode provides high gate fidelity over broadband frequencies. Moreover, excitation of waveguide mode and extraction of quantum dot emission are extremely efficient in this system, and chip-scale integration is possible.

For a PhC W1 waveguide, the dispersion diagram of the fundamental TE-like propagation mode is shown in Fig. 1(a). A divergentlike LDOS and slow group velocity for the fundamental propagating waveguide mode is seen for wavelengths near the PhC waveguide mode cutoff edge [at $0.266(c/a)$, where c is the vacuum speed of light and a is the lattice constant of photonic crystal]. Emission of an emitter embedded in a PhC waveguide, at the field maximum of the localized waveguide mode, exhibits a large spontaneous emission enhancement proportional to $1/(v_g V_{\text{eff}})$, where v_g is the group velocity and V_{eff} is the effective mode volume per unit cell for a PhC waveguide fundamental mode. Furthermore, a large propagation mode β factor—probability of a photon being emitted into a desired waveguide mode regardless of nonradiative decay of the emitter—is obtained

throughout the entire propagation spectrum.⁷ Figure 1(b) shows a schematic of the system, with a three-level emitter. The ground and excited states, $|g\rangle$ and $|e\rangle$, respectively, are coupled via h -polarization photons (corresponding to the waveguide TE mode) with frequency ω_{wg} . A metastable state $|s\rangle$ is decoupled from waveguide modes but is resonantly coupled to $|e\rangle$ via a classical, optical control field with Rabi frequency $\Omega(t)$. Dynamics of the emitter operator σ_- is described by Heisenberg operator equation

$$\frac{d\sigma_-}{dt} = -\frac{1}{2\tau}\sigma_- + i\delta_{\text{ew}}\sigma_- + \kappa a_{\text{in}}. \quad (1)$$

The waveguide output fields a_{out} and b_{out} are related to the input fields by $a_{\text{out}} = a_{\text{in}} + \kappa\sigma_-$ and $b_{\text{out}} = b_{\text{in}} + \kappa\sigma_-$. $1/\tau = 1/\tau_{\text{SE}} + 1/\tau_{\text{NR}} + 1/\tau'$ is the total decay rate of the emitter, in which $1/\tau_{\text{SE}} = \text{PF}/\tau_0$ is the emitter's spontaneous emission

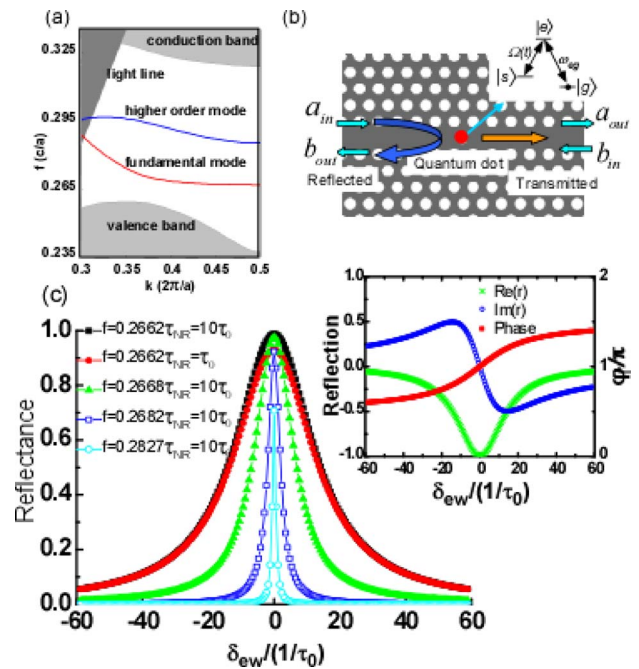


FIG. 1. (Color online) (a) PhC waveguide band structure within the TE-like band gap. Both fundamental and a higher order mode are shown. Structure parameters: $r=0.275a$, $h=0.5a$, $\epsilon=12$ and $a=420$ nm. (b) Schematic of a single incident photon interacts with a near resonant QD. (c) Reflectance as a function of normalized QD detuning frequencies for different normalized PhC waveguide frequencies with QD $\tau_{\text{NR}}=10\tau_0$ and $\tau_{\text{NR}}=\tau_0$. Inset: reflection coefficient (real part and imaginary part) and phase when $f=0.2662$, $\tau_{\text{NR}}=10\tau_0$.

^{a)}Author to whom correspondence should be addressed. Electronic addresses: jg2499@columbia.edu and cww2104@columbia.edu.

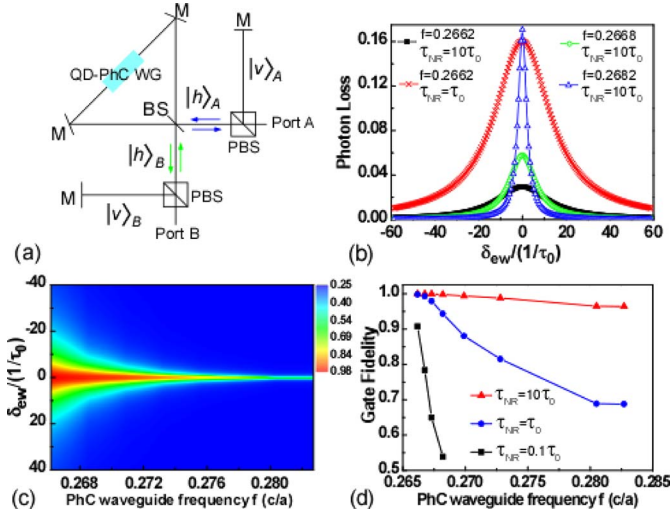


FIG. 2. (Color online) (a) Schematic setup of CPF gate with Sagnac loop. (b) Gate photon loss as a function of normalized QD detuning frequencies for CPF gate operated at different PhC waveguide frequencies with QD $\tau_{NR} = 10\tau_0$ and $\tau_{NR} = \tau_0$. (c) Gate fidelity for different detuning frequencies and PhC waveguide frequencies ($\tau_{NR} = 10\tau_0$) (d) CPF gate fidelity as a function of normalized PhC waveguide frequencies with QDs $\tau_{NR} = 10\tau_0$, $\tau_{NR} = \tau_0$ and $\tau_{NR} = 0.1\tau_0$.

rate in the PhC waveguide (where PF is the Purcell factor and $1/\tau_0$ is the emitter decay rate in bulk material), $1/\tau_{NR}$ is the nonradiative decay rate and $1/\tau'$ is related to the spontaneous emission into a continuum of radiation and/or leaky modes. δ_{ew} and κ are, respectively, the frequency detuning and coupling coefficient between emitter and waveguide mode, and $\kappa = 1/\sqrt{2}\tau_{SE}$. We use the calculated β factors in Ref. 7 [defined as $\beta = (1/\tau_{SE}/1/\tau_{SE} + 1/\tau')$] and consider the QD τ_0 to be 1 ns, and the nonradiative decay to be subgigahertz at low temperature.¹⁰ Figure 1(c) shows the reflectance $R (=|r|^2 = |b_{out}/a_{in}|^2)$ as a function of normalized QD detuning frequencies. The waveguide frequencies f are normalized to c/a . Figure 1(c) shows that the reflectance curve is spectrally broadened with maximum reflectance close to unity when the waveguide mode approaches slower group velocities. Nonradiative recombination of the QD as a loss mechanism is also shown here for the case of $\tau_{NR} = \tau_0$, where the maximum reflectance peak is decreased. The inset of Fig. 1(c) shows numerically calculated reflection coefficient when $f = 0.2662$. It indicates that $r \approx -1$ when the QD is on resonance with the waveguide mode with a slow group velocity of $\sim c/154$. An input photon is nearly perfectly reflected by the single QD, and simultaneously gets a π -phase shift. Similar reflection properties have also suggested in surface plasmon nanowires,⁶ and Ref. 11 describes the ideal waveguide case.

Based on the QD-PhC waveguide system described above, we can adopt the protocol of Duan and Kimble (see Ref. 3). However, here we consider a more compact schematic setup as shown in Fig. 2(a) to realize a CPF gate between input photon A (target qubit) and input photon B (control qubit). Generally the input photon state A or B can be described as $(|h\rangle + |v\rangle)/\sqrt{2}$ and, after the polarization beam splitter (PBS), only $|h\rangle_A$ mode or $|h\rangle_B$ mode enters at the 50:50 beam splitter (BS) and couples into the PhC waveguide from both sides simultaneously. After traveling through the Sagnac loop, the photon recombines at the BS and exits the system from the same port it entered. Moreover,

using the 50:50 BS transformation matrix,¹² the $|h\rangle_A$ mode and $|h\rangle_B$ mode will gain a π -phase difference with respect to each other when they leave the Sagnac loop and we denote this effect as $|h\rangle_A \xrightarrow{\text{Sagnac}} |h\rangle_A$, $|h\rangle_B \xrightarrow{\text{Sagnac}} -|h\rangle_B$. We note that the optical paths and propagation loss for $|h\rangle$ and $|v\rangle$ components can be stably tuned experimentally to be identical. All these free space light paths can also be integrated onto a single chip.

The implementation of the CPF gate between photons A and B thereby consists of three steps in the protocol. We first show, in ideal case, the initial and final states of the QD-photon system to illustrate the states evolution after each step.

- (1) First we initialize the emitter in ground state and apply a control field $\Omega(t)$ simultaneous with the arrival of single photon B. The control field (properly chosen to be impedance matched¹³) will result in capture of the incoming single photon while inducing QD state flips from $|g\rangle$ to $|s\rangle$:

$$|h\rangle_B |g\rangle_{\text{QD}} \rightarrow |\text{vac}\rangle_B |s\rangle_{\text{QD}}, \quad |v\rangle_B |g\rangle_{\text{QD}} \rightarrow |v\rangle_B |g\rangle_{\text{QD}}, \quad (2)$$

where we used $|\text{vac}\rangle_B$ to describe the h -polarized B photon after storage.

- (2) Next we send photon A into the system. Only when emitter is on ground state $|g\rangle$ will the QD-waveguide system reflect photon $|h\rangle_A$ and introduce a π -phase shift on this photon simultaneously. The whole system will result in four possible states as follows below:

$$\begin{aligned} |h\rangle_A |\text{vac}\rangle_B |s\rangle_{\text{QD}} &\rightarrow |h\rangle_A |\text{vac}\rangle_B |s\rangle_{\text{QD}}, \\ |v\rangle_A |\text{vac}\rangle_B |s\rangle_{\text{QD}} &\rightarrow |v\rangle_A |\text{vac}\rangle_B |s\rangle_{\text{QD}}, \end{aligned} \quad (3)$$

$$|h\rangle_A |v\rangle_B |g\rangle_{\text{QD}} \rightarrow -|h\rangle_A |v\rangle_B |g\rangle_{\text{QD}},$$

$$|v\rangle_A |v\rangle_B |g\rangle_{\text{QD}} \rightarrow |v\rangle_A |v\rangle_B |g\rangle_{\text{QD}}.$$

- (3) Finally we can choose the same $\Omega(-t)$ to drive the emitter from $|s\rangle$ back to $|g\rangle$, and retrieve single photon $|h\rangle_B$ as a time reversal process of (1). The retrieval process can be expressed as $|\text{vac}\rangle_B |s\rangle_{\text{QD}} \rightarrow |h\rangle_B |g\rangle_{\text{QD}}$. The retrieval photon generated in PhC waveguide is exactly the same as the input photon in (1), but it will get a π -phase change when it leaves the BS.

$$\begin{aligned} |h\rangle_A |\text{vac}\rangle_B |s\rangle_{\text{QD}} &\rightarrow -|h\rangle_A |h\rangle_B |g\rangle_{\text{QD}}, \\ |v\rangle_A |\text{vac}\rangle_B |s\rangle_{\text{QD}} &\rightarrow -|v\rangle_A |h\rangle_B |g\rangle_{\text{QD}}, \\ -|h\rangle_A |v\rangle_B |g\rangle_{\text{QD}} &\rightarrow -|h\rangle_A |v\rangle_B |g\rangle_{\text{QD}}, \\ |v\rangle_A |v\rangle_B |g\rangle_{\text{QD}} &\rightarrow |v\rangle_A |v\rangle_B |g\rangle_{\text{QD}}. \end{aligned} \quad (4)$$

After these three steps, the state of input photons can thus be described by

$$\begin{aligned} |\varphi\rangle_{\text{initial}} &= |h\rangle_A |h\rangle_B + |v\rangle_A |h\rangle_B + |h\rangle_A |v\rangle_B + |v\rangle_A |v\rangle_B \\ \Rightarrow |\varphi\rangle_{\text{ideal}} &= -|h\rangle_A |h\rangle_B - |v\rangle_A |h\rangle_B - |h\rangle_A |v\rangle_B + |v\rangle_A |v\rangle_B. \end{aligned} \quad (5)$$

This ideal photon state evolution demonstrates the completed implementation of controlled phase-flip gate operation. The

emitter is not entangled with the photon states and returns to the original ground state after the gate operation.

We emphasize the importance of the Sagnac loop in our scheme. Because QD emission couples into both left- and right-propagation waveguide modes, if we have incident $|h\rangle_A$ mode only from one side of the waveguide in step (2), we cannot combine these two modes later into a single output without loss because they are entangled with the QD. The advantage of using the Sagnac loop here is to remove the entanglement between the waveguide left- and right-propagating modes and the QD, by having $|h\rangle_A$ mode incident from both sides of the waveguide. Thus we can get single output $-|h\rangle_A$ (when QD state is $|g\rangle$) or $|h\rangle_A$ (when QD state is $|s\rangle$).

Furthermore we discuss the storage and retrieval process in steps (1) and (3). We need coherent storage and retrieval of a single photon $|h\rangle_B$ and the store/retrieval efficiency degrades the quality of the control phase gate. In our case, the optimal storage strategy in (1) is splitting the incoming pulse and having it incident from both sides of the emitter simultaneously, which is the time reversal process of a single photon generation. There is a one-to-one correspondence between the incoming pulse shape and the optimal field $\Omega(t)$. The retrieval process in (3) is time reversal process of the storage process in (1) and both efficiencies are theoretically determined by the calculated reflection/transmission coefficient.^{6,14} Reversible transfer of coherent light to and from the internal state of a single trapped atom in a cavity has already been demonstrated in experiment¹⁵ and the efficiency could improve up to 90%.

Next we consider nonideal cases which include frequency mismatch between emitter and waveguide mode, nonradiative decay of the emitter, experimentally achievable values of low group velocities, as well as photon storage and retrieval efficiency. We include in Fig. 2(b) all the above loss mechanisms and experimental limitations into the photon loss during the gate operation. Not surprisingly the gate loss decreases to very low level when we operate at the slow-light PhC waveguide frequencies and the gate loss increases when the nonradiative decay of the QD is comparable to the radiative decay. Fidelity of the CPF gate, described by $|\langle\varphi_{\text{ideal}}|\varphi_{\text{actual}}\rangle|$, measures the difference between the actual output photon state and the ideal [Eq. (5)] state. We note that the PhC waveguide mode propagation loss and the insertion loss do *not* decrease the gate fidelity. Figure 2(c) shows how the QD-waveguide CPF gate fidelity changes with normalized frequency detuning $\delta_{\text{ew}}/(1/\tau_0)$ and waveguide mode frequency. In addition, in Fig. 2(c), the decrease in the gate fidelity with increasing frequency mismatch indicates the requirement of the input photon frequency (waveguide mode frequency) to be on resonant with the QD transition. However, the frequency matching here is not as stringent as the cavity cases because of the broad spectral range of the propagating PhC waveguide mode. Figure 2(d) shows the QD-waveguide CPF gate fidelity as a function of PhC waveguide mode frequencies (on resonance with QD). When $f=0.2662$, $\nu_g \approx c/154$ have been measured experimentally.¹⁶ Spontaneous emission rate is enhanced by PF=30 and leads to β factor nearly 0.998 for a QD located at the field antinodes with the same dipole orientation as the mode polarization.⁷ The reflectance peak is as high as 0.988 and leads to a gate fidelity up to 0.9999 with $\tau_{\text{NR}}=10\tau_0$. When $f=0.2827$, the PF

tends toward 1 with normal waveguide group velocity yet gate fidelity remains above 0.96. Although the Purcell factor is very low in this case, the reason of the high fidelity is that the QD emissions into free space or other leaky modes are highly suppressed inside the PhC band gap and the one-dimensional waveguide, and thus we have a large β factor (>0.9) maintained throughout the waveguide mode spectral range [~ 10 THz from Fig. 1(a)]. Compared to cavity-assisted schemes in which Lorentzian shape resonance features are involved, the gate operation bandwidth in waveguide-assisted system is much larger. For example, as long as the QD transition is within ~ 2 THz (15 nm) above the waveguide cutoff frequency, our scheme always gets fidelity greater than 0.99 as well as gate loss smaller than 0.18. Moreover even with a QD with 50% quantum yield ($\tau_{\text{NR}} = \tau_0$), the gate fidelity still remains higher than 0.9 within ~ 2 THz bandwidth. Combining the contribution both from Purcell factor and large β factor, our QD-PhC waveguide system has a distinctive advantage compared to cavity-assisted schemes by relaxing the frequency matching condition by approximately two orders of magnitude or more.

In summary we have proposed a scheme to realize quantum control phase-flip gate between two photons through photon-QD interaction in a PhC waveguide. Strong optical confinement and low group velocity in PhC waveguide contributes to the high gate fidelity (~ 0.99) over a tremendous broadband region (~ 2 THz). In our scheme, excitation and extraction can be extremely efficient and chip-scale integration is possible. All these advantages show QD-PhC waveguide system is very promising to be a critical component in quantum information processing.

The authors thank X.D. Yang and J.F. McMillan for helpful discussions. We acknowledge funding support from NSF, DARPA, and NYSTAR.

¹J. McKeever, A. Boca, A. D. Boozer, R. Miller, J. R. Buck, A. Kuzmich, and H. J. Kimble, *Science* **303**, 1992 (2004).

²Y. F. Xiao, J. Gao, X. Yang, R. Bose, G. C. Guo, and C. W. Wong, *Appl. Phys. Lett.* **91**, 151105 (2007).

³L.-M. Duan and H. J. Kimble, *Phys. Rev. Lett.* **92**, 127902 (2004).

⁴E. Waks and J. Vuckovic, *Phys. Rev. Lett.* **96**, 153601 (2006).

⁵J. F. McMillan, M. Yu, D.-L. Kwong, and C. W. Wong, CLEO/QELS, San Jose, California, May 2008, Paper No. QMI6.

⁶D. E. Chang, A. S. Sorensen, E. A. Demler, and M. D. Lukin, *Nat. Phys.* **3**, 807 (2007).

⁷V. S. C. Manga Rao and S. Hughes, *Phys. Rev. B* **75**, 205437 (2007); *Phys. Rev. Lett.* **99**, 193901 (2007).

⁸R. Bose, X. Yang, R. Chatterjee, J. Gao, and C. W. Wong, *Appl. Phys. Lett.* **90**, 111117 (2007).

⁹E. Viasnoff-Schwoob, C. Weisbuch, H. Benisty, S. Olivier, S. Varoutsis, I. Robert-Philip, R. Houdre, and C. J. M. Smith, *Phys. Rev. Lett.* **95**, 183901 (2005).

¹⁰W. Langbein, P. Borri, U. Woggon, V. Stavarache, D. Reuter, and A. D. Wieck, *Phys. Rev. B* **70**, 033301 (2004).

¹¹J. T. Shen and S. Fan, *Opt. Lett.* **30**, 15 (2005).

¹²R. A. Campos, B. E. A. Saleh, and M. C. Teich, *Phys. Rev. A* **40**, 1371 (1989).

¹³J. I. Cirac, P. Zoller, H. J. Kimble, and M. Mabuchi, *Phys. Rev. Lett.* **78**, 3221 (1997).

¹⁴A. V. Gorshkov, A. Andre, M. Fleischhauer, A. S. Sorensen, and M. D. Lukin, *Phys. Rev. Lett.* **98**, 123601 (2007).

¹⁵A. D. Boozer, A. Boca, R. Miller, T. E. Northup, and H. J. Kimble, *Phys. Rev. Lett.* **98**, 193601 (2007).

¹⁶Y. A. Vlasov, M. O. Boyle, H. F. Hamann, and S. J. McNab, *Nature (London)* **438**, 65 (2005).